




## PRECLINICAL REPORTS

# Photo-mediated ultrasound therapy for the treatment of retinal neovascularization in rabbit eyes

Yu Qin PhD<sup>1,2</sup>  | Yixin Yu MD<sup>3,4,5</sup> | Julia Fu<sup>3</sup> | Mingyang Wang<sup>1</sup>  |  
Xinmai Yang PhD<sup>6</sup> | Xueding Wang PhD<sup>1</sup> | Yannis M. Paulus MD<sup>1,3</sup> 

<sup>1</sup>Department of Biomedical Engineering, University of Michigan, Ann Arbor, Michigan, USA

<sup>2</sup>Institute of Acoustics, School of Physics Science and Engineering, Tongji University, Shanghai, China

<sup>3</sup>Department of Ophthalmology and Visual Sciences, University of Michigan, Ann Arbor, Michigan, USA

<sup>4</sup>Eye Center of Xiangya Hospital, Central South University, Changsha, Hunan Province, China

<sup>5</sup>Hunan Key Laboratory of Ophthalmology, Changsha, Hunan Province, China

<sup>6</sup>Institute for Bioengineering Research and Department of Mechanical Engineering, University of Kansas, Lawrence, Kansas, USA

## Correspondence

Xinmai Yang, PhD, Learned Hall, University of Kansas, KS 66045, USA.  
Email: xmyang@ku.edu

Xueding Wang, PhD, 2200 Bonisteel Blvd, University of Michigan, MI 48109, USA.  
Email: xdwang@umich.edu

Yannis M. Paulus, MD, FACS, 1000 Wall St, University of Michigan, MI 48105, USA.  
Email: ypaulus@med.umich.edu

## Funding information

Alliance for Vision Research; National Institutes of Health, Grant/Award Numbers: 1K08EY027458, 1R01EY029489, 1R41EY031219; Alcon Research Institute Young Investigator Grant; Vision Research Core Center of National Eye Institute, Grant/Award Number: P30EY007003; Research to Prevent Blindness

## Abstract

**Objectives:** Retinal neovascularization (RNV) is the growth of abnormal microvessels on the retinal surface and into the vitreous, which can lead to severe vision loss. By combining relatively low-intensity ultrasound and nanosecond-pulse-duration laser, we developed a novel treatment method, namely photo-mediated ultrasound therapy (PUT), which holds a potential to remove RNV with minimal or no damage to the adjacent tissues.

**Methods:** RNV was created in both albino and pigmented rabbits ( $n = 10$ ) through a single intravitreal injection with DL- $\alpha$ -amino adipic acid. RNV was treated with PUT 8 weeks postinjection. After PUT treatment, animals were evaluated longitudinally for up to 6 weeks. Treatment outcomes were evaluated through fundus photography, red-free fundus photography, fluorescein angiography (FA), and histopathology.

**Results:** In both albino and pigmented rabbits, there were no leakage in the treatment area immediately after PUT treatment as demonstrated by FA, indicating the cessation of blood perfusion of the RNV in the treated area. The fluorescence leakage did not recover in albino rabbits during the 6-week posttreatment monitoring period, and only  $9.9 \pm 9.8\%$  of the neovascularization remained at the end of 6 weeks. In the pigmented rabbits, the fluorescence leakage partially returned, but the level of leakage decreased over time during the 6-week posttreatment monitoring period, and only  $10.8 \pm 9.8\%$  of the neovascularization remained at the end of 6 weeks. Histology demonstrated removal of vasculature without damage to the surrounding neurosensory retina.

**Conclusions:** These results demonstrate that PUT could precisely remove RNV without damage to the surrounding neurosensory retina in both rabbit strains.

## KEYWORDS

angiogenesis, laser, photo-mediated ultrasound therapy, retinal neovascularization, ultrasound

Yu Qin and Yixin Yu contributed equally to this study.

This is an open access article under the terms of the Creative Commons Attribution-NonCommercial License, which permits use, distribution and reproduction in any medium, provided the original work is properly cited and is not used for commercial purposes.

© 2022 The Authors. *Lasers in Surgery and Medicine* published by Wiley Periodicals LLC.

## INTRODUCTION

Retinal neovascularization (RNV) is the formation of abnormal new blood vessel on the retinal surface and into the vitreous, leading to plasma leakage, hemorrhage, and potential for severe vision loss.<sup>1</sup> RNV is a cause of vision loss in many diseases, including diabetic retinopathy—a leading cause of vision loss among working-age adults, with approximately 2.6 million people visually impaired in 2015 from diabetes.<sup>2</sup> RNV is also implicated in other ischemic retinopathies such as retinopathy of prematurity, sickle cell retinopathy, and retinal vein occlusions.<sup>1</sup>

Treatment of RNV includes anti-vascular endothelial growth factor (VEGF) therapy and laser therapy. While the use of anti-VEGF therapies has revolutionized the treatment of ocular neovascularization, anti-VEGF therapy could potentially lead to retinal atrophy, and blockage of VEGF-A during retinal stress could lead to accelerated retinal cell death and is an area of active investigation.<sup>3–12</sup> In addition, 15%–40% of eyes fail to or only partially respond to anti-VEGF therapies.<sup>13</sup> Further, anti-VEGF therapy involves frequent, often monthly, intravitreal injections of anti-VEGF agents, which are costly and inconvenient for patients, and carry a risk of eye infection or endophthalmitis.<sup>14</sup> Nonpharmacological therapies used in treatment of RNV include panretinal photocoagulation (PRP).<sup>15</sup> In a recent study which examined PRP treatment outcomes after a 12-month period for 77 patients with high-risk proliferative diabetic retinopathy, reduction in RNV from the baseline was only observed in 70.5% of patients. Complete RNV regression was only observed in 25% of patients. Possible complications of PRP include worsening of diabetic macular edema, vitreous hemorrhage, tractional retinal detachment, and elevation in intraocular pressure.<sup>16</sup>

We have developed a novel, noninvasive, agent-free, and highly selective treatment method termed photo-mediated ultrasound therapy (PUT). This therapeutic method utilizes relatively low-intensity ultrasound bursts, which is spatially and temporally synchronized with nanosecond duration laser pulses.<sup>17–22</sup> By temporally synchronizing the nanosecond laser pulse to the rarefactional peak pressure of the ultrasound burst, and spatially overlaying the laser and ultrasound beams, PUT can promote cavitation activity in specifically targeted microvessels.<sup>23</sup> Specifically, PUT is designed to maximize the mechanical effect of cavitation while the related thermal effect is minimized by careful selection of ultrasound and laser parameters. The mechanical effects resulted from the oscillation of cavitation bubbles within these microvessels include microjets and shear stresses.<sup>24</sup> The produced mechanical stresses can potentially affect the physiological functions of platelets, endothelial cells, and erythrocytes, leading to hemorrhage, blood clot formation, and vasoconstriction.<sup>21</sup>

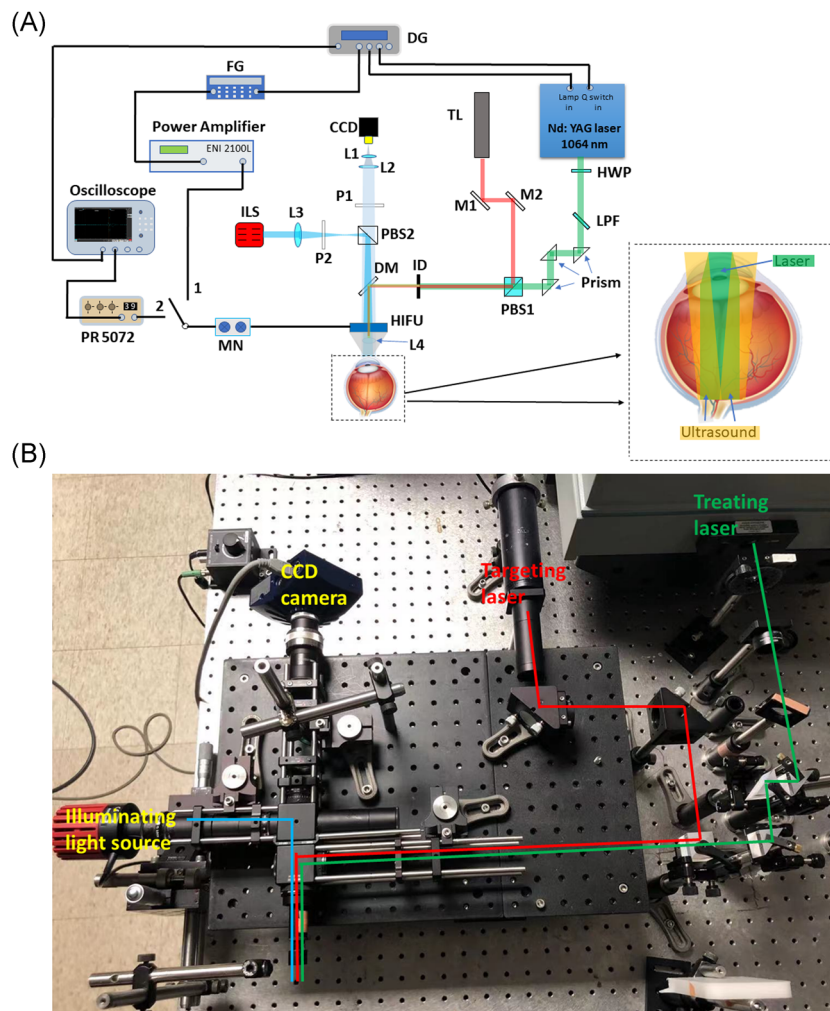
Previously, we demonstrated the efficacy of PUT in safely removing neovascularization in both the choroid and the cornea of rabbit eyes.<sup>21–23,25</sup> In this study, PUT was applied to the treatment of RNV for the first time. The feasibility of PUT for RNV was tested via experiments on a DL-AAA induced RNV model in both New Zealand white (NZW) rabbits and Dutch Belted pigmented (DBP) rabbits, and the safety was evaluated by histology.

## MATERIALS AND METHODS

### PUT system

Figure 1 shows the schematic Figure 1A and a photograph Figure 1B of the PUT system for treatment of rabbit RNV in vivo. A standard Nd:YAG laser (Continuum Powerlite DLS 8010) was used as the laser source for the treatment, which provided 1064-nm light at a pulse repetition rate of 10 Hz and pulse width of 5 nanoseconds. The treatment laser beam, which was filtered by a long-pass filter to remove the residual 523-nm light and only keep the 1064-nm light, was directed to the sample with its energy before the rabbit sclera measured by a Nova PE25BB-SH-V2 pyroelectric head (Ophir Optronics Ltd.). Considering that the 1064 nm wavelength light would be attenuated 40% in the rabbit eye before reaching the retina,<sup>26</sup> the laser energy was compensated accordingly so that the desired light radiant exposure level would be achieved at the retina. To control the beam size at the retina, the collimated laser beam was slightly focused onto the front focal plane of the rabbit eye using objective lens L4. The laser beam would then be collimated again by the eye's optics as a result of this design. The laser spot size was adjusted to 3 mm in diameter on the retinal layer by controlling the size of an iris diaphragm. The therapeutic ultrasound system consisted of a function generator (DS345; Stanford Research System), an RF power amplifier (2100 L; ENI), a matching network (Impedance Matching Network H-107; Sonic Concepts), and a HIFU transducer (center frequency 0.5 MHz, H-107; Sonic Concepts). The system provided 0.5 MHz ultrasound burst with 5% duty cycle at a pulse repetition rate of 10 Hz. The HIFU transducer had a geometric focal distance of 63.2 mm, a focal depth of 21.42 mm, and a focal width of 3.02 mm. The ultrasound pressure was calibrated in a euthanized rabbit eye at the appropriate position on the retinal using a standard needle hydrophone (Onda HNC-1500). A pulse delay generator (Model DG355; Stanford Research Systems) with a precision within 1 picosecond was employed to provide triggers for the laser and the ultrasound systems with a repetition rate of 10 Hz. Both the laser power and the synchronization between laser pulses and ultrasound bursts could be adjusted through the pulse delay

**FIGURE 1** System schematic. (A) System schematic for PUT treatment of rabbit RNV in vivo. (B) Photograph of the PUT system. CCD, charge-coupled device; DG, delay generator; DM, dichroic mirrors; FG, function generator; HIFU, high-intensity focused ultrasound; HWP, half-wave plate; ID, iris diaphragm; ILS, illuminating light source; L1–L4, lens; LPF, long-pass filter; M1&M2, mirror; MN, matching network for HIFU transducer; P1&P2, polarizer; PBS1&PBS2, polarizing beam-splitter; PR, pulser-receiver; PUT, photo-mediated ultrasound therapy; RNV, retinal neovascularization; TL, targeting laser



generator. Each laser pulse was precisely synchronized at the rarefactional phase of the ultrasonic wave (i.e., in-phase setting). It can be achieved by measuring the traveling time of a laser-induced photoacoustic wave propagating from the target sample to the HIFU transducer as described previously.<sup>23,25,27</sup> To ensure the accuracy of measurement, the laser system outputted a 532 nm laser instead of 1064 nm during the measurement procedure, benefiting from the strong optical absorption of hemoglobin at 532 nm. When the switch in Figure 1A was connected to the position “2,” the produced photoacoustic signal can be received by the HIFU transducer, then amplified by a pulser/receiver (PR 5072; Olympus), and finally displayed on an oscilloscope (TDS540; Tektronix). When the switch was connected to the position “1,” the HIFU transducer would be ready for the treatment.

A charge-coupled device (CCD) was applied to monitor the treatment effect in real-time and its illumination light was provided by a mounted LED (Wavelength 565 nm, M565L3; Thorlabs). The illumination light beam was expanded by a convex lens, then reflected by a polarizing beam splitter, and finally merged

with the therapeutic laser beam and directed to the rabbit eye fundus. A HeNe laser (Wavelength 632.8 nm, HNL020LB; Thorlabs) was used to provide an aiming beam to align the therapeutic laser beam. The aiming beam allowed the identification of the exact treatment location on the retina through the CCD. A custom-built, three-dimensional printed cone was attached to the ultrasound transducer, and filled with agar-gelatin (2 g/100 ml agar and 1.25 g/100 ml gelatin) based couplant to provide acoustic coupling. A middle hole was left in the center of the cone for the optical lens (L4) fixation and light propagation including the therapeutic laser beam, the guiding beam, and the illumination light beam. The ultrasound and therapeutic laser beams were aligned in advance. A good acoustic coupling can be monitored by examining the amplitude of the received photoacoustic signal.

## Experimental animal care and handling

NZW rabbits (2.5–3.0 kg, 3–8 months old, both genders) and DBP rabbits (2.0–2.5 kg, 3–8 months old, both

genders) were involved in this study. The reason why we selected these two strain rabbits is the eye condition of NZW and DBP rabbits are similar to the oculocutaneous albinism patients and normal human beings, respectively. It can ensure the applicability of this technology to all patients. The animals were housed in an air-conditioned room with a 12-hour light–dark cycle, fed standard laboratory food, and allowed free access to water. All the animal handling procedures were carried out in compliance with protocols approved by the Institutional Animal Care and Use Committee (IACUC) at the University of Michigan (Protocol number PRO00 008567, PI Paulus), with strict adherence to the ARVO Statement for the Use of Animals in Ophthalmic and Vision Research.

To induce anesthesia and analgesia, rabbits were initially sedated with a combination of ketamine hydrochloride 40 mg/kg (Ketalar; Par Pharmaceutical Co., Inc.) and xylazine 5 mg/kg (Anased; MWI/VetOne) given intramuscularly (IM), and proparacaine was used as a topical anesthesia. The subsequent anesthesia was maintained with 2% isoflurane in pure oxygen using a V-Gel<sup>®</sup> (D10004; Jorgensen Laboratories). The rabbit pupils were dilated with topical application of phenylephrine hydrochloride 2.5% and tropicamide 1% eye drops. A V8400D Capnograph & SpO<sub>2</sub> Digital Pulse Oximetry (MWI Animal Health) was used to continuously monitor the heart rate and blood oxygenation to assess anesthetic levels. Every 15 minutes, the rectal temperature was taken and utilized to regulate a water-circulating heating pad (TP-700; Stryker Corporation) to maintain a stable body temperature.

### Induction of RNV model

The DL- $\alpha$ -aminoadipic acid (DL-AAA) induced RNV model in rabbits was used as described previously.<sup>28,29</sup> DL-AAA (Sigma) was dissolved in 1 N hydrochloric acid to form a 120 mg/ml stock solution. The pH was adjusted with sodium hydroxide to 7.4. The stock solution was diluted to an 80 mM solution using sterile saline. The final solution was filtered through a disposable Millex-GP syringe filter unit with a pore size of 0.22  $\mu$ m (Batch, MK-BL8989; Sigma-Aldrich Corp.) to remove any potential particulates before intraocular injection. Solutions were made immediately before use and all solutions remained at room temperature until time of injection. Five NZW rabbits ( $n=5$  eyes) and five DBP rabbits ( $n=5$  eyes) were used as RNV models by intravitreal injection of DL-AAA under anesthesia. RNV was induced with a single intravitreal injection of 80 mM DL-AAA solution with an injection site at 10 o'clock position for the right eye and 2 o'clock position for the left eye. The volume of the DL-AAA injected was 80  $\mu$ l for NZW rabbits and 50  $\mu$ l for DBP rabbits. The density of the induced RNV became stable 8 weeks after the

injection of DL-AAA,<sup>28</sup> and thus 8 weeks was selected as the time point for treatment with PUT. This DL-AAA model was selected since it has been shown to result in stable, long-term RNV. Eight weeks was selected as the time point for PUT treatment post-RNV model creation due to the stability of RNV at this time point to ensure that changes noted in RNV were due to the treatment.

### Evaluation method

A digital fundus camera (Topcon 50EX Fundus Camera and Digital Imaging System; Topcon) was used to take fundus photos, red-free fundus photos, and fluorescein angiography (FA) photos of the animal eye before and after PUT treatment. The change in retinal morphology and structure was monitored using fundus photography. With the addition of a green filter, red-free fundus photography was used to observe superficial lesions and some vascular anomalies inside the retina and surrounding tissue. FA was performed to evaluate the blood perfusion of the retina and the fluorescein leakage of RNV by injecting 0.1 ml/kg of fluorescein sodium (100 mg/ml; Akorn Inc.) intravenously into the marginal ear vein. The rabbit was euthanized with a lethal dose of pentobarbital (Euthanasia 390 mg/ml pentobarbital and 50 mg phenytoin, 0.22 mg/kg; Intervet Inc.) intravenously into the marginal ear vein at the end of each experiment, along with the removal of a critical organ.

### Image processing and quantification of vascular leakage area

The RNV intensity was evaluated by quantifying the fluorescence leakage area in the late phase of FA. The treatment region was segmented manually according to the treatment laser targeted area using Adobe Illustrator CC 2018 software. For DBP rabbits, the fluorescence leakage area was measured by image analysis based on the brightness of fluorescence leakage using open-source software (ImageJ). The number of pixels included was used to calculate the fluorescence leakage area. The method used to obtain the leakage area was published previously by our group and demonstrated to be quantitative and repeatable.<sup>28</sup> There are three steps to this method. The segmented image is first transformed to 8-bit grayscale, after which various spots on the fluorescence leakage area are selected. The gray value of these spots is then used to threshold the processed image. The vascular bed is then extracted from the image using a vessel identifier method. Finally, the number of pixels in this area is counted and the progress is tracked longitudinally over time. The fluorescence leakage area is more difficult to quantify for NZW rabbits than DBP rabbits. This is because the contrast of the leakage between the background fluorescein is low in NZW due



to the diffuse choroidal leakage of fluorescein that is blocked in DBP rabbits, as previously reported.<sup>28</sup> The fluorescence leakage area in NZW rabbits was measured by tracing over the hyperfluorescent leakage on late-phase FA with a paintbrush tool and counting how many pixels were covered. This course of action provides the extracted leakage area from the vasculature network. All the fluorescence leakage areas of these two strain rabbits were normalized by pretreatment (8 weeks after DL-AAA injection) pixels. We analyzed at least three eyes with long-term leakage and without any ocular complication in each strain for each quantification data point.

### Histological analysis of retina

One NZW rabbit and one DBP rabbit without any treatment were euthanized at 8 weeks after DL-AAA intravitreal injection. One NZW rabbit and one DBP rabbit were euthanized at 7 days after PUT treatment. Three NZW rabbits and three DBP rabbits from the PUT group were euthanized at 45 days after PUT treatment. The eye was enucleated immediately and fixed in a 10% formalin solution for 48 hours before being maintained in 70% ethanol until processing. The eyecup containing the treated area was split into numerous representative strips with a thickness of 5 mm after the anterior segment of the eye, lens, and vitreous humor were removed. The strips were all prefixed in 4% agar before being embedded in paraffin. The paraffin-embedded sections (thickness 5  $\mu$ m) were obtained with a microtome and stained with hematoxylin and eosin (H&E). These sections were analyzed under a light microscope (Olympus BX-51). Photographs were taken with a digital camera (Olympus DP70).

### Statistical analysis

Differences in the fluorescence leakage in all the posttreatment groups were compared to before-treatment groups independently using *t* tests with SPSS software. Benjamini–Hochberg correction was performed on all statistical analyses. Differences were considered statistically significant when  $p < 0.05$ . Sample size for statistical power of the quantification results was performed using G\*Power software with  $\alpha = 0.05$ . In the NZW rabbit group, all the statistical powers are larger than 0.9 (the conventional desired power is 0.8<sup>30</sup>). In the DBP rabbit group, only the statistical powers of 2 days and 1 week are smaller than 0.8, which are 0.26 and 0.44 respectively; the statistical powers of the rest of the time points are all larger than 0.9. We find that only three rabbits are need because PUT results in a significant, measurable treatment change.

## RESULTS

### Efficiency of PUT treatment

Four NZW rabbits (one eye in each rabbit), in which RNV were induced by intravitreal injection of DL-AAA, were treated with a single PUT session with 85 mJ/cm<sup>2</sup> laser fluence at 1064 nm and 0.48 MPa ultrasound pressure at 0.5 MHz at the retina for 10 min. The green circles in Figure 2, with 3-mm diameter, indicate the treatment area covering the RNV and choroidal vessels. Immediately after PUT treatment, the choroidal vessels in the treatment area became hazy without obvious hemorrhage (Figure 2B1), and the treated RNV was unidentifiable in both fundus (Figure 2B1) and red-free (Figure 2B2) images. Further, hypofluorescence was demonstrated throughout the entire FA (early phase, middle phase, and late phase) with sharp margins without an overlying lesion or hemorrhage on the fundus imaging indicating nonperfusion/hypoperfusion as the cause of the hypofluorescence. The region of hypofluorescence gradually reduced over time, as shown in Figure 2B3–B5. This delayed FA filling time indicates that the blood flow speed in the treatment area was slower than that in the normal vessel immediately after the PUT treatment. Areas of nonperfusion were also observed in the targeted region. The RNV intensity is usually proportional to the size of the fluorescence leakage area in the late phase of the FA. Compared with before treatment, only  $0.5 \pm 0.3\%$  of the fluorescence leakage remain in the late phase of the FA image, demonstrating that the blood vessels in the RNV area may have either stopped perfusion, reduced in size, or were removed immediately after the PUT treatment. Following the treatment, the fluorescence leakage did not recover in the treated region during the 6-week monitoring period. This indicates that RNV was removed effectively by PUT, and the treatment effect was sustained for at least 6 weeks, as shown in Figure 2C5–H5. However, some of the choroidal vessels in the treatment region, which were not our target, were also removed.

The limitation of the current NZW rabbit RNV model is that NZW rabbits do not have melanin pigmentation within the retinal pigment epithelium (RPE) layer between the choroidal and retinal blood vessels, whereas significant melanin pigment exists within the RPE layer in most human eyes. Therefore, four DBP rabbits, which have melanin within the RPE layer similar to most human eyes, were used to induce RNV through intravitreal injection of DL-AAA with the same protocol as done in the NZW rabbits. Eight weeks after the DL-AAA injection (Figure 3A1–A5), RNV in DBP rabbits was treated by PUT with the same parameters as done in the NZW rabbits, which was 85mJ/cm<sup>2</sup> laser fluence at 1064 nm and 0.48 MPa ultrasound pressure at 0.5 MHz at retina for 10 minutes.

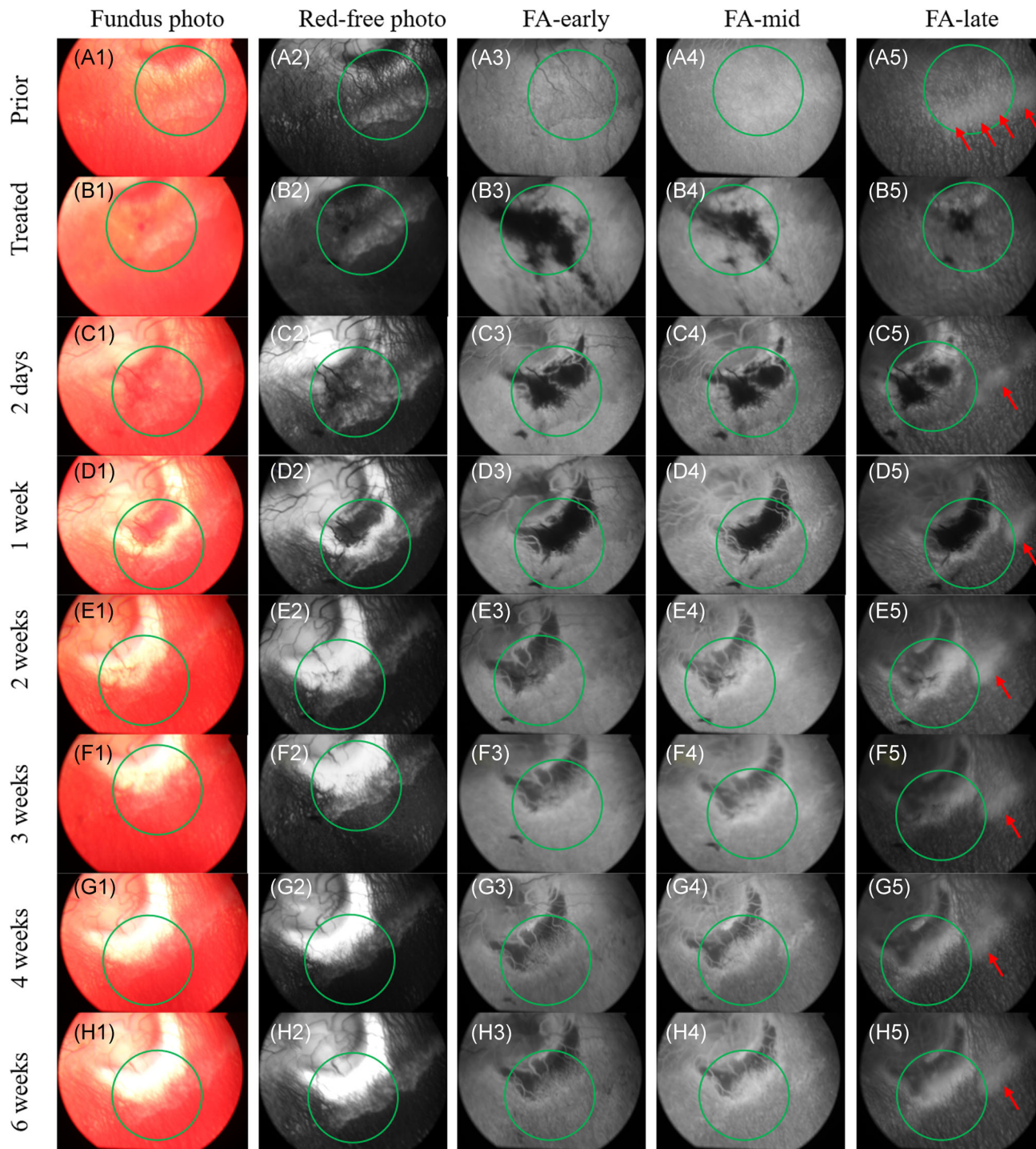


**FIGURE 2** Representative fundus photographs (A1–H1), red-free images (A2–H2), and fluorescein angiography (FA) of NZW rabbits' RNV with single PUT treatment. (A3–H3): Early phase FA. (A4–H4): Middle phase FA. (A5–H5): Late phase FA. In these images, the extensive leakage (red arrow) indicated the region of RNV. Prior: 1 day before the PUT treatment (8 weeks after intravitreal DL-AAA injection). Treated: immediately after the PUT treatment. Two days: 2 days after PUT treatment. \* weeks: \* weeks after PUT treatment (\* = 1, 2, 3, 4, 6). The green circles indicate the PUT treatment area. The applied ultrasound pressure was 0.48 MPa at 0.5 MHz, the applied laser radiant exposure was 85 mJ/cm<sup>2</sup> at 1064 nm, and the treatment duration was 10 min. DBP, Dutch Belted pigmented; DL-AAA, DL- $\alpha$ -aminoadipic acid; NZW, New Zealand white; PUT, photo-mediated ultrasound therapy; RNV, retinal neovascularization

Immediately after PUT treatment, most of the RNV region had a cessation of perfusion along with a minor hemorrhage, as shown in Figure 3B1–B5. Two days after PUT treatment, the minor hemorrhage was absorbed

and the RNV region was reperfused with a stronger fluorescence leakage than before PUT treatment (prior), as shown in Figure 3C1–C5 at approximately 60% of the initial leakage area at 2 days and 1 week, which are more



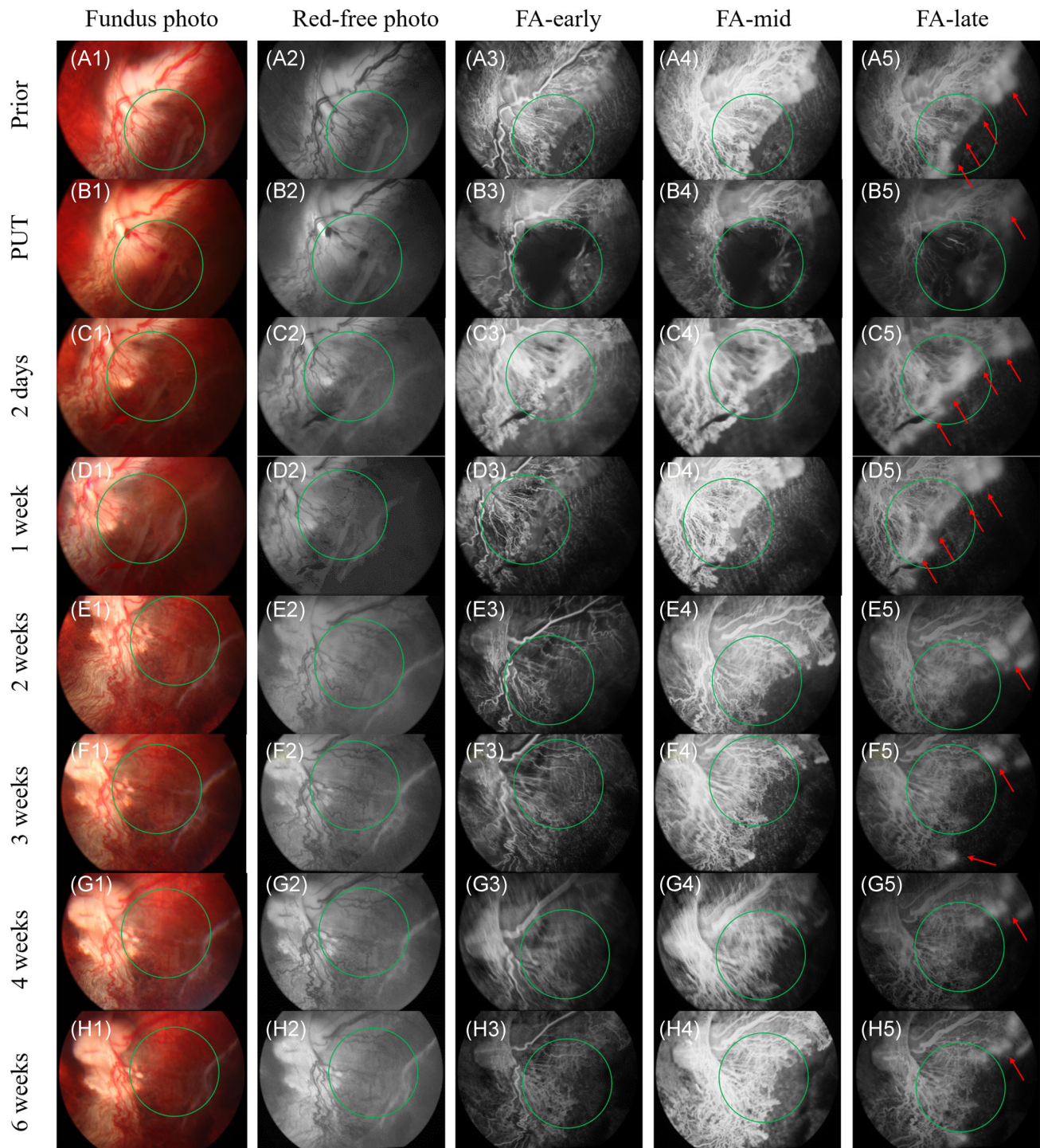


**FIGURE 3** Representative fundus photographs (A1–H1), red-free images (A2–H2), and fluorescein angiography (FA) of DBP rabbits' RNV with single PUT treatment. (A3–H3): Early phase FA. (A4–H4): Middle phase FA. (A5–H5): Late phase FA. In these images, the extensive leakage (red arrow) indicated the region of RNV. Prior: 1 day before the PUT treatment (8 weeks after intravitreal DL-AAA injection). PUT: immediately after the PUT treatment. Two days: 2 days after PUT treatment. \* weeks: \* weeks after PUT treatment (\* = 1, 2, 3, 4, 6). The green circles indicate the PUT treatment area. The applied ultrasound pressure was 0.48 MPa at 0.5 MHz, the applied laser radiant exposure was 85 mJ/cm<sup>2</sup> at 1064 nm, and the treatment duration was 10 minutes. DBP, Dutch Belted pigmented; DL-AAA, DL- $\alpha$ -amino adipic acid; NZW, New Zealand white; PUT, photo-mediated ultrasound therapy; RNV, retinal neovascularization

than that noted with NZW rabbits. In Figure 35–G5, the late phase of FA showed a clear trend of decreasing fluorescence leakage from Weeks 1 to 6 after PUT treatment, indicating the gradual resolution of the

treated RNV. Only  $10.8 \pm 9.8\%$  of the fluorescence leakage remained at 6 weeks after PUT.

The fluorescence leakage of the late phase of FA was quantified to quantitatively evaluate the treatment

efficiency in both NZW rabbits and DBP rabbits, as shown in Figure 4. In both rabbit strains, PUT can stop the perfusion of RNV immediately after treatment, resulting in only  $0.5 \pm 0.3\%$  and  $0.5 \pm 0.1\%$  of fluorescence leakage in NZW rabbits and DBP rabbits, respectively. At 2 days after PUT, the perfusion in the majority of the RNV region was not recovered in NZW rabbits, with only  $5.2 \pm 6.5\%$  of fluorescence leakage remaining in comparison with that of before PUT. In DBP rabbits, however, a larger percentage of the RNV region was initially reperfused with  $60.7 \pm 47.4\%$  of fluorescence leakage remaining in comparison with that of before PUT at 2 days which was similar to the value at 1 week. During the following weekly observation from Weeks 1 to 6 after PUT, the fluorescence leakage of NZW rabbits was in a stable range between  $15.3 \pm 17.2\%$  (1 week after PUT) and  $7.6 \pm 7.9\%$  (4 weeks after PUT). Only  $9.9 \pm 9.8\%$  of the fluorescence leakage remained at 6 weeks after PUT treatment, indicating that only  $9.9 \pm 9.8\%$  of RNV remained perfused. In DBP rabbits, although RNV reperfusion happened, the fluorescence leakage decreased gradually from  $60.1 \pm 30.7\%$  (1 week after PUT) to  $10.8 \pm 9.8\%$  (6 weeks after PUT). These quantification results further demonstrated that PUT is effective for RNV treatment in both NZW rabbits and DBP rabbits.

### Histology safety evaluation

To examine the safety of PUT, H&E histology staining was performed to evaluate possible damage to the neurosensory retina. Two rabbits (one NZW rabbit and one DBP rabbit) were euthanized before treatment (8 weeks after DL-AAA injection) and at 1 week after PUT treatment. Three NZW rabbits and three DBP rabbits were euthanized at 6 weeks after PUT treatment. Representative histology samples are shown in Figure 5.

As described in our previous study of DL-AAA induced RNV rabbit model,<sup>28</sup> histological sections from H&E stains of the retina of these rabbits demonstrated extensive retinal atrophy and thinning in both DBP and NZW rabbits. The retina of DL-AAA induced RNV rabbit model could be classified into two discrete regions: moderate retinal atrophy areas and severe, full-thickness retinal atrophy areas. In both NZW (Figure 5A–C) and DBP rabbits (Figure 5G–I) moderate retinal atrophy regions, every retina layer existed but demonstrated significant thinning but intact organization. In DBP rabbits, the severe, full-thickness retinal atrophy areas (Figure 5J–L) showed disorganized nuclei remaining within the regions, and the inner retina, specifically the ganglion cell layer (GCL) demonstrated hyperpigmentation. In NZW rabbits, the severe, full-thickness retinal atrophy areas (Figure 5D–F) demonstrated extensive atrophy within every layer of the retina with significant disorganization. Only disorganized nuclei of reduced density which could represent portions of the GCL, inner nuclear layer, and outer nuclear layer with reduced nuclei density remained within the severe, full-thickness retinal atrophy regions. Of note, every retinal layer's characteristics were similar to those seen before PUT treatment. The retina atrophy and thinning in the H&E histology were caused by DL-AAA, similar to the results published previously,<sup>28</sup> and no significant additional changes was induced by PUT treatment. Figure 5B,E demonstrates that some hemorrhage appeared in the choriocapillaris/choroid layer adjacent to the RPE in NZW rabbits at 1 week after PUT. However, the hemorrhage disappeared at 6 weeks after PUT, as shown in Figure 5C,F. No hemorrhage was observed in DBP rabbits. H&E histology results demonstrated that PUT resulted in no visible morphologic changes in the neurosensory retina at 1 and 6 weeks after treatment in both atrophic areas in both strains.

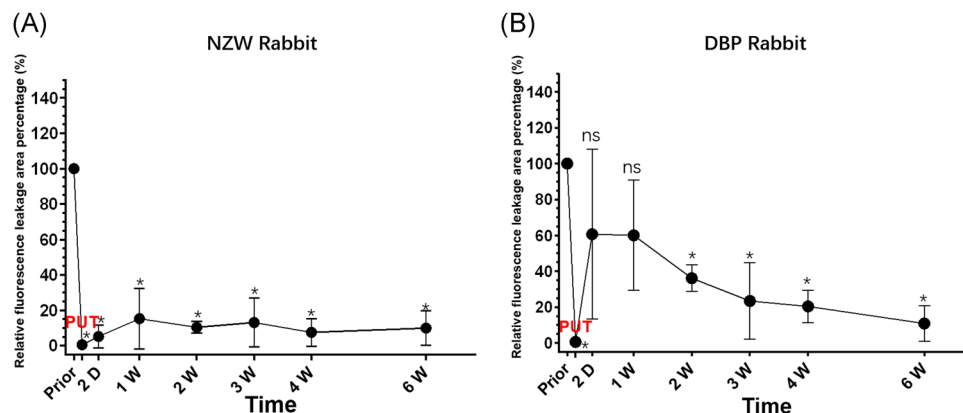


**FIGURE 4** Quantification of the normalized fluorescence leakage area in the PUT treatment of NZW rabbits ( $n = 3$ ) and DBP rabbits ( $n = 3$ ) at different time points after treatment. 2 D, 2 days after PUT; # W, # weeks after PUT (# = 1, 2, 3, 4, 6). Compared to before treatment (prior), \* is for statistically significant difference, and “ns” is for no statistically significant difference. DBP, Dutch Belted pigmented; NZW, New Zealand white; PUT, photo-mediated ultrasound therapy



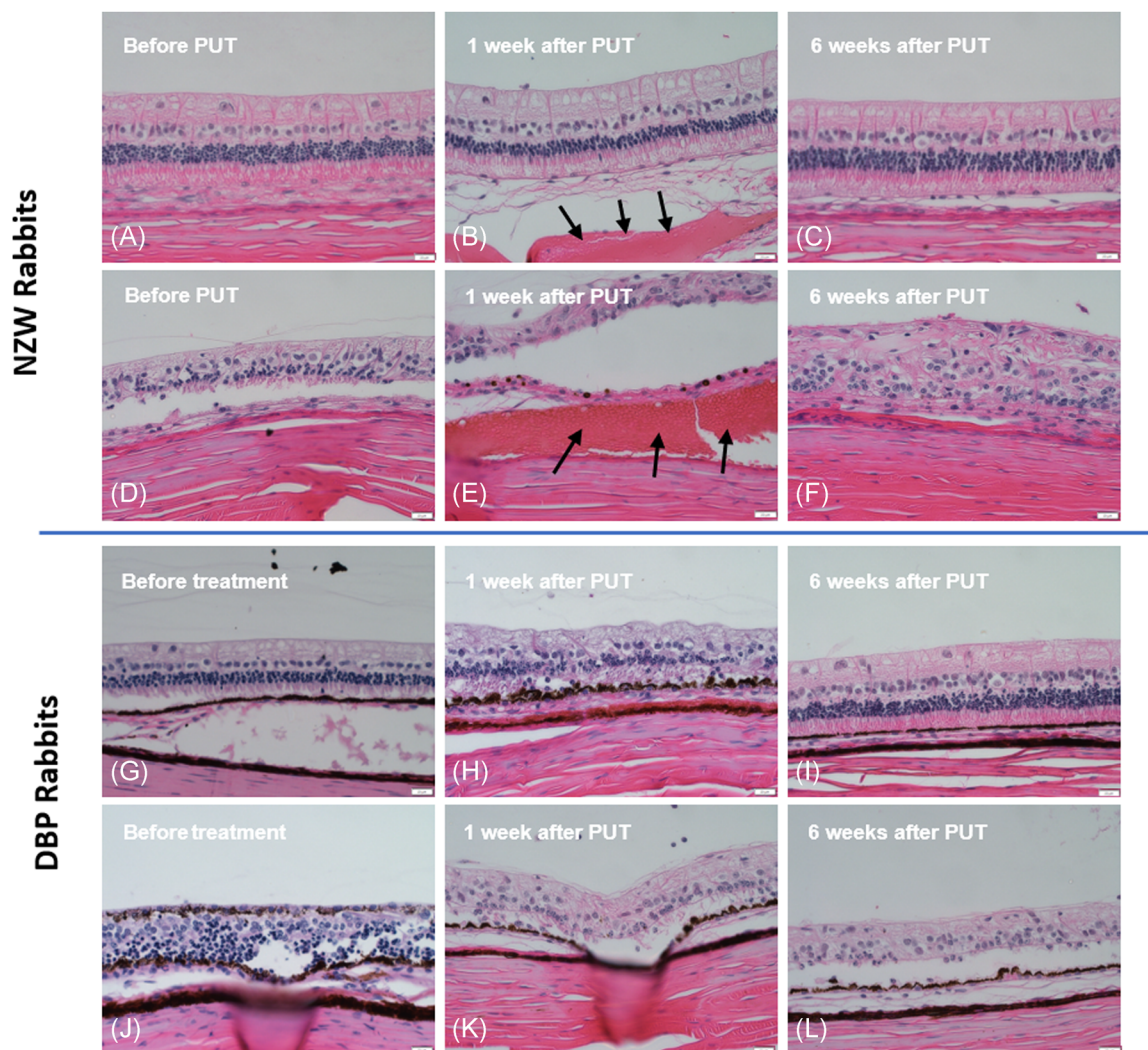


**FIGURE 5** Structural characteristics of the New Zealand white (NZW) rabbits' retina (A–F) and Dutch Belted pigmented (DBP) rabbits' retina (G–L). H&E staining histology of retina before PUT treatment (after IVT of DL-AAA for 8 weeks) (A, D, G, J), at 1 week after PUT treatment (B, E, H, K), and at 6 weeks after PUT treatment (C, F, I, L) ( $\times 40$  amplification). (A–C, G–I) were taken from the moderate retinal atrophy region noted with the DL-AAA model. (D–F, J–L) were taken from the severe, full-thickness retinal atrophy region of the retina noted with the DL-AAA model. Black arrows indicate hemorrhage between the retina and choroid layer. In NZW rabbit, histological sections at these two-time points after PUT treatment demonstrated no change in the neurosensory retina, only temporary hemorrhage between retina and choroid layer appeared at 1 week after PUT but disappeared at 6 weeks after PUT. In DBP rabbit, while the DL-AAA model produced abnormal retinal appearance before PUT treatment, histological sections at these two-time points after PUT treatment demonstrated no change in the neurosensory retina after PUT treatment. Bar = 20  $\mu\text{m}$ . DL-AAA, DL- $\alpha$ -aminoacidic acid; H&E, hematoxylin and eosin; PUT, photo-mediated ultrasound therapy

## CONCLUSION AND DISCUSSION

This study demonstrates for the first time the feasibility of PUT for the treatment of RNV. With a single session, PUT can remove RNV effectively in both NZW rabbits and DBP rabbits with only  $9.9 \pm 9.8\%$  and  $10.8 \pm 9.8\%$  of RNV remaining in NZW rabbits and DBP rabbits, respectively, at 6 weeks after PUT treatment. The results showed a side effect in treating the RNV of NZW rabbits, which is some of the choroidal vessels in the treatment region could be removed, but not in the treatment of DBP rabbits. Safety evaluation based on histology demonstrated temporary choroidal hemorrhage that appeared at 1 week

and disappeared at 6 weeks after PUT in NZW rabbits, while no hemorrhage was observed in DBP rabbits. In NZW rabbits, because there is no pigment in the RPE and choroidal layers, laser energy can be delivered to the choroidal vessels more readily than in DBP rabbits in which melanin absorbs the laser. In one of our previous studies of PUT in normal NZW rabbits,<sup>21</sup> no morphological damage was observed in any layer of the retina at either 24 or 72 hours after PUT, but possible blood clots were noticed in the treated choroidal blood vessels at 24 hours after PUT. The choroidal hemorrhage noted in NZW rabbits in this study may be caused by the different parameters of laser and ultrasound compared to the

previous study in which only blood clots were noted in choroidal vessels.<sup>21</sup> In humans, pigment exists in the RPE and choroidal layer except for oculocutaneous albinism patients.<sup>31</sup> DBP rabbit eyes, with parameters similar to most human beings, demonstrated no damage to the neurosensory retina after PUT (Figure 5G–L). For oculocutaneous albinism patients, however, the short-term safety (choroidal hemorrhage) and the long-term safety (choroidal vessel removal) of PUT may be a concern.

PUT is based on the cavitation effect induced by the synchronized nanosecond laser pulses and ultrasound bursts. The outcome of PUT treatment depends on the parameters of laser and ultrasound including the wavelength of the laser, the pulse width of the laser, the radiant exposure of the laser, the frequency of the ultrasound, the duty cycles of the ultrasound, the pressure of the ultrasound, and the synchronization between laser and ultrasound.<sup>17,18,20–23,25,27</sup> There is a list of parameters that can be optimized to maximize the treatment efficacy while minimizing the side effects. For example, in the future, we can study how the laser wavelength affects the treatment depth to find the optimal laser wavelength for treating RNV, such that we may avoid the side effect of removing the choroidal vessels in NZW rabbits. Some limitations exist in this study, including the DL-AAA animal model. While it results in stable, long-term RNV which is why it was selected for this study, it also results in significant retinal atrophy which does not mimic human RNV disorders and limits the ability of this study to evaluate safety due to the retinal atrophy noted on histopathology from the DL-AAA model.

In conclusion, PUT was able to precisely eliminate RNV without causing injury to the surrounding neurosensory retina in both NZW and DBP rabbits utilizing a synchronized 1064 nm nanosecond pulse laser and a 0.5 MHz ultrasonic burst. However, a part of the choroidal vessels was removed when treating the RNV in NZW rabbits. Further optimization in the laser and ultrasound parameters will be needed to improve the safety of PUT in the future.

## ACKNOWLEDGMENTS

This study is supported in part by NIH 1R01EY029489 (XY), NIH 1K08EY027458 (YMP), NIH 1R41EY031219 (YMP), the Alliance for Vision Research (YMP), the Alcon Research Institute Young Investigator Grant (YMP), and unrestricted departmental support from Research to Prevent Blindness (YMP). This study utilized the Vision Research Core Center funded by P30EY007003 from the National Eye Institute. The authors would like to thank Dr. Yuqing Chen and the Center for Advanced Models and Translational Sciences and Therapeutics (CAMTraST) at the University of Michigan Medical School for the generous donation of the rabbits used in this study.

## CONFLICTS OF INTEREST

XY, XW, and YMP serve as inventors on a University of Kansas and University of Michigan patent application on PUT technology and have equity in a company PhotoSonoX LLC.

## ORCID

Yu Qin  <http://orcid.org/0000-0003-4196-9291>

Mingyang Wang  <http://orcid.org/0000-0002-4076-1643>

Yannis M. Paulus  <http://orcid.org/0000-0002-0615-628X>

## REFERENCES

1. Campochiaro PA. Ocular neovascularization. *J Mol Med.* 2013; 91:311–21.
2. Cheloni R, Gandolfi SA, Signorelli C, Odone A. Global prevalence of diabetic retinopathy: protocol for a systematic review and meta-analysis. *BMJ Open.* 2019;9(3):022188.
3. Xu W, Cheng W, Cui X, Xu G. Therapeutic effect against retinal neovascularization in a mouse model of oxygen-induced retinopathy: bone marrow-derived mesenchymal stem cells versus Conbercept. *BMC Ophthalmol.* 2020;20(1):1–8.
4. Nishijima K, Ng YS, Zhong L, Bradley J, Schubert W, Jo N, et al. Vascular endothelial growth factor-A is a survival factor for retinal neurons and a critical neuroprotectant during the adaptive response to ischemic injury. *Am J Pathol.* 2007;171(1):53–67.
5. Foss A, Rotsos T, Empeledis T, Chong V. The development of macular atrophy in patients with wet age-related macular degeneration receiving anti-VEGF treatment. *Ophthalmologica.* Published online 2021. <https://doi.org/10.1159/000520171>
6. Munk MR, Ceklic L, Ebnetter A, Huf W, Wolf S, Zinkernagel MS. Macular atrophy in patients with long-term anti-VEGF treatment for neovascular age-related macular degeneration. *Acta Ophthalmol.* 2016;94(8):e757–64.
7. Gemenetzi M, Lotery A, Patel P. Risk of geographic atrophy in age-related macular degeneration patients treated with intravitreal anti-VEGF agents. *Eye.* 2017;31(1):1–9.
8. Kaynak S, Kaya M, Kaya D. Is there a relationship between use of anti-vascular endothelial growth factor agents and atrophic changes in age-related macular degeneration patients? *Turk J Ophthalmol.* 2018;48(2):81–4.
9. Enslow R, Bhuvanagiri S, Vegunta S, Cutler B, Neff M, Stagg B. Association of anti-VEGF injections with progression of geographic atrophy. *Ophthalmol Eye Dis.* 2016;8:S38863–2.
10. Grunwald JE, Daniel E, Huang J, Ying G, Maguire MG, Toth CA, et al. Risk of geographic atrophy in the comparison of age-related macular degeneration treatments trials. *Ophthalmology.* 2014;121(1):150–61.
11. Horani M, Mahmood S, Aslam TM. Macular atrophy of the retinal pigment epithelium in patients with neovascular age-related macular degeneration: what is the link? Part I: a review of disease characterization and morphological associations. *Ophthalmol Ther.* 2019;8(2):235–49.
12. Horani M, Mahmood S, Aslam TM. A review of macular atrophy of the retinal pigment epithelium in patients with neovascular age-related macular degeneration: what is the link? Part ii. *Ophthalmol Ther.* 2020;9(1):35–75.
13. Wallsh JO, Gallemore RP. Anti-VEGF-resistant retinal diseases: a review of the latest treatment options. *Cells.* 2021;10(5):1049.
14. Paulus YM, Qin Y, Yu Y, Fu J, Wang X, Yang X. Photo-mediated ultrasound therapy to treat retinal neovascularization. Paper presented at: 2020 42nd Annual International Conference of the IEEE Engineering in Medicine & Biology Society (EMBC); 2020.

15. Lin J, Chang JS, Smiddy WE. Cost evaluation of panretinal photocoagulation versus intravitreal ranibizumab for proliferative diabetic retinopathy. *Ophthalmology*. 2016;123(9):1912–8.
16. Figueira J, Fletcher E, Massin P, Silva R, Bandello F, Midena E, et al. Ranibizumab plus panretinal photocoagulation versus panretinal photocoagulation alone for high-risk proliferative diabetic retinopathy (PROTEUS study). *Ophthalmology*. 2018;125(5):691–700.
17. Hu Z, Zhang H, Mordovanakis A, Paulus YM, Liu Q, Wang X, et al. High-precision, non-invasive anti-microvascular approach via concurrent ultrasound and laser irradiation. *Sci Rep*. 2017;7:40243.
18. Li S, Qin Y, Wang X, Yang X. Bubble growth in cylindrically-shaped optical absorbers during photo-mediated ultrasound therapy. *Phys Med Biol*. 2018;63(12):125017.
19. Yang X, Hu Z, Zhang H, Mordovanakis A, Paulus YM, Wang X. Antivascular photo-mediated ultrasound therapy. Paper presented at: 2016 IEEE International Ultrasonics Symposium (IUS); 2016.
20. Yang X, Zhang H, Li J, Paulus Y, Wang X. The application of antivascular photo-mediated ultrasound therapy in removing microvessels in the eye. Paper presented at: 2017 IEEE International Ultrasonics Symposium (IUS); 2017.
21. Zhang H, Xie X, Li J, Qin Y, Zhang W, Cheng Q, et al. Removal of choroidal vasculature using concurrently applied ultrasound bursts and nanosecond laser pulses. *Sci Rep*. 2018;8(1):1–10.
22. Zhang W, Qin Y, Xie X, Hu Z, Paulus YM, Yang X, et al. Real-time photoacoustic sensing for photo-mediated ultrasound therapy. *Opt Lett*. 2019;44(16):4063–6.
23. Qin Y, Yu Y, Xie X, Zhang W, Fu J, Paulus YM, et al. The effect of laser and ultrasound synchronization in photo-mediated ultrasound therapy. *IEEE Trans Biomed Eng*. 2020;67:3363–70.
24. Singh R, Wang X, Yang X. Cavitation induced shear and circumferential stresses on blood vessel walls during photo-mediated ultrasound therapy. *AIP Adv*. 2020;10(12):125227.
25. Qin Y, Yu Y, Fu J, Xie X, Wang T, Woodward MA, et al. Photo-mediated ultrasound therapy for the treatment of corneal neovascularization in rabbit eyes. *Transl Vis Sci Technol*. 2020;9(13):16–6.
26. Algerey PV, Torstensson P, Tengroth B. Light transmittance of ocular media in living rabbit eyes. *Invest Ophthalmol Visual Sci*. 1993;34(2):349–54.
27. Wang M, Qin Y, Wang T, Orringer JS, Paulus YM, Yang X, et al. Removing subcutaneous microvessels using photo-mediated ultrasound therapy. *Lasers Surg Med*. 2020;52(10):984–92.
28. Yu Y, Qin Y, Fu J, Li Y, Zhang W, Zhu T, et al. Long-term multimodal imaging characterization of persistent retinal neovascularization using DL-alpha-aminoadipic acid in pigmented and white rabbits. *Exp Eye Res*. 2021;207:108577.
29. Cao J, MacPherson TC, Iglesias BV, Liu Y, Tirko N, Yancopoulos GD, et al. Aflibercept action in a rabbit model of chronic retinal neovascularization: reversible inhibition of pathologic leakage with dose-dependent duration. *Invest Ophthalmol Visual Sci*. 2018;59(2):1033–44.
30. Cohen J. Statistical power analysis. *Curr Dir Psychol Sci*. 1992;1(3):98–101.
31. Gronskov K, Ek J, Brondum-Nielsen K. Hypophosphatasia. *Orphanet J Rare Dis*. 2007;2:43.

**How to cite this article:** Qin Y, Yu Y, Fu J, Wang M, Yang X, Wang X, et al. Photo-mediated ultrasound therapy for the treatment of retinal neovascularization in rabbit eyes. *Lasers Surg Med*. 2022;54:747–757. <https://doi.org/10.1002/lsm.23539>